JOURNAL OF MATERIALS SCIENCE 26 (1991) 3356–3361

A study of the effects of chloride salt treatment on the properties of hypereutectoid steels

D. MUKHERJEE
RDCIS, SAIL, Ranchi, India

A. K. CHAKRABARTI
Metallurgical Engineering Department, IIT, Kharagpur 721 302, India

NaCl and $CaCl_2$ additions to liquid hypereutectoid steel cause appreciable removal of inclusions. A small amount of graphitization also occurs due to this treatment. While the low-temperature impact properties of the steel improve appreciably following NaCl treatment, $CaCl_2$ treatment leads to deterioration of these properties.

1. Introduction

The effect of NaCl and chlorine gas treatment of liquid steels has been investigated in the past [1–4]. Russian research [2] has documented the beneficial effects of treatment of liquid steel with halide salts on inclusion removal and degassing. The effects of NaCl treatment on the microstructure and mechanical properties of low-carbon steels (0.2–0.25 wt % C) have been revealed further through large-scale plant trials [3]. It was reported earlier that both NaCl and Cl_2 gas treatments cause graphitization in steels [3, 4]. In addition, NaCl treatment improves certain mechanical properties by reducing the inclusion content in steel. As part of a continuing programme, the present investigation was undertaken to evaluate the effect of NaCl and $CaCl_2$ treatments on the structure and properties of hypereutectoid steels.

2. Experimental procedure

Liquid steel (1.0 wt % C) melted in a 100 kg magnesium-lined induction furnace was tapped in 30-kg batches in a magnesium-lined ladle, where it was treated separately with 1 wt % each of $CaCl_2$ and NaCl, respectively. It was then and cast in the form of 62 mm square billets in metal moulds and 150 mm round bars in sand moulds. The cast samples were coded as follows:

Treatment	150 mm round bar	62 mm square billet
None	1A	1B
$CaCl_2$(1 wt %)	2A	2B
NaCl (1 wt %)	3A	3B

After cropping off the top portions, the billets were hot forged into 19 mm diameter rods. The chemical analysis of the samples is given in Table I.
The following tests were carried out.

2.1. Dilatometry

The eutectoid transformation temperatures of the salt-treated and untreated samples were determined by thermogravimetric analysis (TMA). The heating rate was 10 °C min^{-1} from room temperature to 850 °C.

2.2. Estimation of inclusion content

To study whether the inclusion content has any effect on the mechanical properties of these steels, it was estimated using image analysis after diamond polishing samples from 1B, 2B and 3B.

2.3.

The microstructures of the cast samples and the machined chips were examined. The cast samples were then examined in a Jeol microprobe analyser to detect precipitation of graphite.

2.4.

The physical characteristics of the underside of chips from the three steels formed at a cutting speed of approximately 120 m min^{-1} depth of cut 1.5 mm, and feed 0.1 mm min^{-1}, were examined under the SEM. As-forged samples of all the steels were furnace-cooled after austenitization at 900 °C for 1 h. Grain size in the annealed samples was determined by comparing the microstructures with standard ASTM charts at magnification ×100.

2.5. Heat treatment

In order to evaluate the effect of salt treatment on the response to quench-tempering treatment, samples (12 mm diameter × 12 mm length) of the steels were quenched from 800 °C and tempered isochronally at temperatures in the 200–700 °C range for 1 h. The progress of tempering was followed by hardness measurements and microstructural examination.

0022–2461/91 $03.00 + .12

TABLE I Chemical analysis of samples

Sample no.	Sample code	Analysis (%)					
		C	Mn	Si	S	P	Al
1	1A	0.89	0.38	0.017	0.013	0.028	0.05
2	2B	0.92	0.38	0.013	0.014	0.042	0.0021
3	3B	0.92	0.38	0.010	0.014	0.034	0.0068

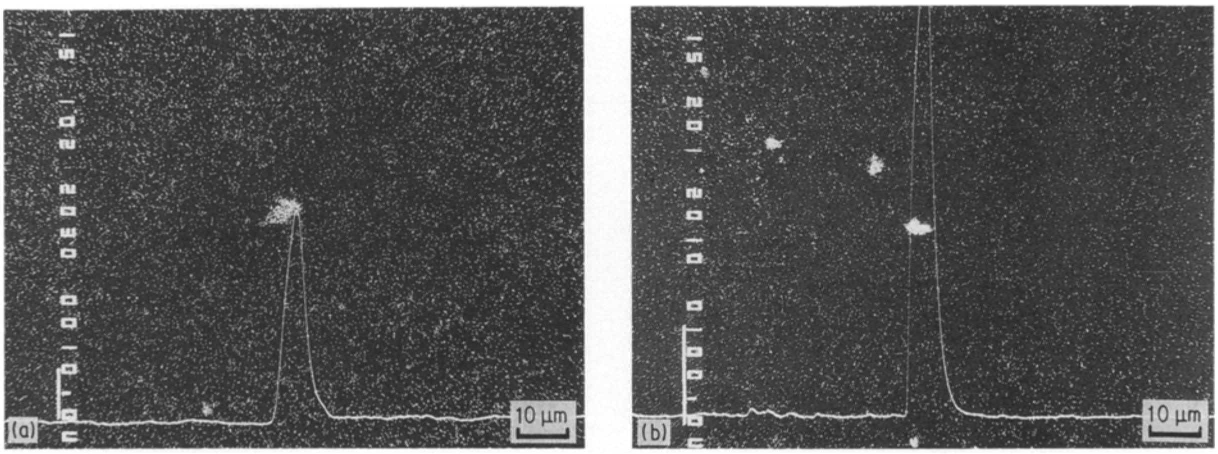

Figure 1 SEM of graphite with superimposed $CK\alpha$ map in (a) cast steel 3B and (b) cast, quenched and tempered steel 3B (oil-quenched from 900 °C and tempered at 700 °C).

2.6. Evaluation of mechanical properties

Two series of tests were carried out. Firstly tensile test samples were prepared from longitudinal sections in the as-forged condition, as well as after full annealing from 800 °C. In the second series, the as-forged bars were first normalized at 880 °C for 1 h. The bars were then forged to strips at around 900 °C. The strips were lightly rolled at around 700–800 °C to give parallel faces. From these strips, samples for tensile and impact tests were made. Strip thickness was around 4.5 mm.

Fracture surfaces of the as-forged tensile samples were examined under the SEM.

3. Results

The as-cast microstructure of steel 3B revealed evidence of graphite precipitation which was confirmed by electron microprobe analysis (Fig. 1a). The graphite particles were also detected in the cast, quenched and tempered samples (Fig. 1b). The matrices of as-cast and annealed samples of all the steels had the usual lamellar pearlite microstructure. But complete

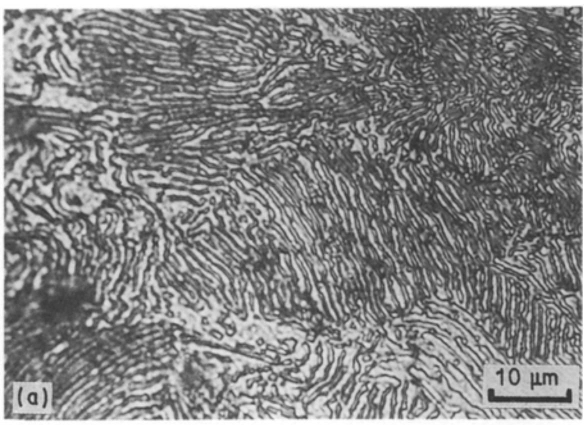

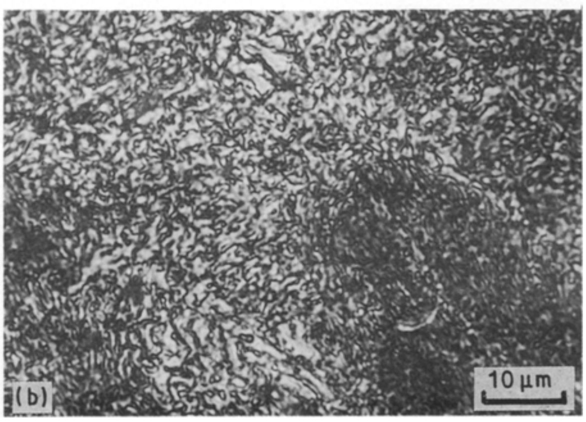

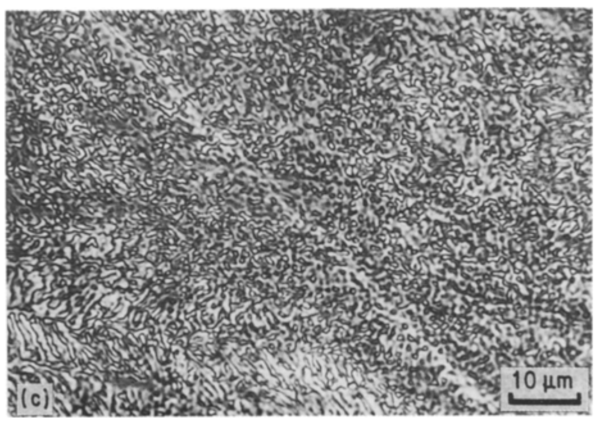

Figure 2 Microstructures of chips of as-cast bars of (a) steel 1A; (b) 2A; (c) 3A. Cutting speed, 66 m min^{-1}.

TABLE II Physical properties

Steel	Average volume fraction of inclusions	Critical temperature (°C)		
		A_1^a	A_{cm}^a	Specific resistance ($\times 10^{-3}$ mm)
1B	0.549	770	790	163.73
2B	0.281	745	775	166.09
3B	0.253	755	780	155.75

[a] A_1 and A_{cm} are not absolute but relative vlaues, with the conditions for the tests of 1A, 2A, 3A remaining identical.

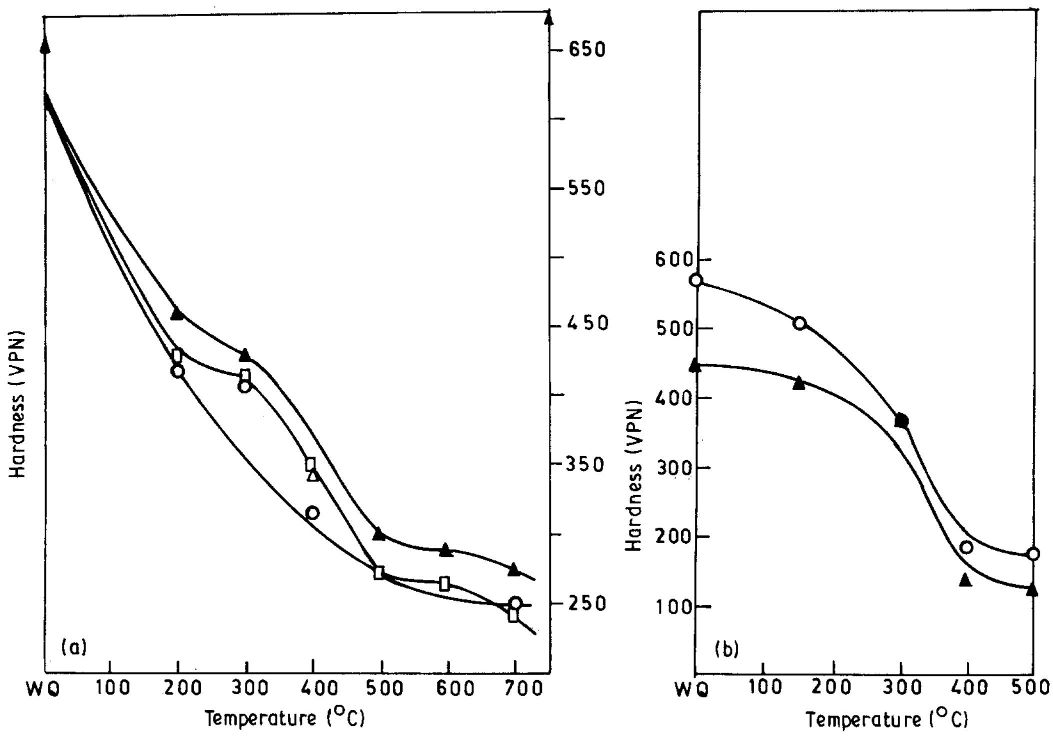

Figure 3 Isochronal tempering curves of (a) forged and (b) cast steels. Quenched from 800 °C. ○, 1B; □, 2B; ▲, 3B.

TABLE III Results of tensile tests on as-forged and annealed samples

Steel	Treatment	Hardness (VPN)	UTS (kg mm^{-2})	Elongation (%)	Reduction in area (%)
1B	Hot-forged	335	88.17	6.0	15.35
2B	Hot-forged	270	79.07	1.07	4.9
3B	Hot-forged	248	74.60	5.4	12.12
1B	annealed from 775 °C	–	87.54	9.5	12.11
2B	775 °C	–	85.68	5.4	5.88
3B	775 °C	–	68.89	14.7	27.43

spheroidization of pearlite in the as-forged and air-cooled condition occurred in steel 3B. On the other hand, the untreated steel 1A developed the usual lamellar pearlite structure in the as-forged and air-cooled condition. The matrix microstructure consisted of partially spheroidized pearlite in $CaCl_2$-treated steel 2B after similar treatment. On lowering the annealing temperature to 775 °C, steel 3B developed a spheroidized structure. Differences in the degree of spheroidization were also noted in the microstructures of the chips formed during machining of the as-cast 150 mm bars. Chips of steel 1A had a lamellar pearlite structure (Fig. 2a), whereas the microstructure of steel 3A consisted of fully spheroidized carbides (Fig. 2c). The chips of steel 2A had a partially spheroidized structure (Fig. 2b).

NaCl treatment had a grain refining effect which could be appreciated by comparing the prior austenite grain size in samples annealed from 900 °C. ASTM grain size decreased from no. 4 in steel 1A to no. 6 in steel 2A, and then to no. 7 in steel 3A. There was only a small change in the transformation temperatures AC_1 and AC_m following salt treatment (Table II) and only a marginal difference in the tempering behaviour

TABLE IV Tensile properties of strip samples

Steel	Direction	YS ($kg\ mm^{-2}$)	Average YS	UTS ($kg\ mm^{-2}$)	Average UTS	Elongation (%)	Average Elongation (%)
	Longitudinal	59.23		96.24		8.0	
			61.6		97.96		6.8
	Longitudinal	63.97		99.68		5.6	
1B	Transverse	–		109.28		13.11	
	Transverse	85.77	84.82	100.04	103.05	12.22	9.18
	Transverse	83.86		99.84		12.22	
	Longitudinal	58.33		93.88		9.4	
			57.89		93.14		8.7
	Longitudinal	57.74		92.39		8.0	
2B	Transverse	–		68.49		6.11	
	Transverse	–	–	70.03	65.06	6.88	5.25
	Transverse	–		56.65		2.77	
	Longitudinal	61.81		93.05		8.24	
			62.15		93.97		8.12
		62.5		94.88		8.0	
3B	Transverse	90.03		102.08		11.11	
	Transverse	88.24	88.73	101.89	102.19	6.11	9.44
	Transverse	87.93		102.59		11.11	

TABLE V Impact strength of strip samples (standard specimen 55 × 10 × 2.5 mm)

Steel	Room temperature (24 °C)			0 °C			– 20 °C		
	Joules	$J\ cm^{-2}$	Average $J\ cm^{-2}$	Joules	$J\ cm^{-2}$	Average $J\ cm^{-2}$	Joules	$J\ cm^{-2}$	Average $J\ cm^{-2}$
	0.952	4.72		0.952	4.47		0.544	2.81	
1B	0.952	4.65	4.67	0.816	4.06	4.36	0.544	2.68	2.28
	0.952	4.65		0.952	4.55		0.272	1.34	
	0.68	3.47		0.408	2.08		0.136	0.68	
2B	0.952	4.69	4.94	0.952	4.67	3.35	0.136	0.804	1.60
	1.36	6.66		0.68	3.31		0.68	3.34	
	0.952	4.57		0.952	4.84		0.816	4.05	
3B	0.952	4.61	4.61	0.952	4.76	4.76	0.952	4.76	4.52
	0.952	4.65		0.952	4.69		0.952	4.76	

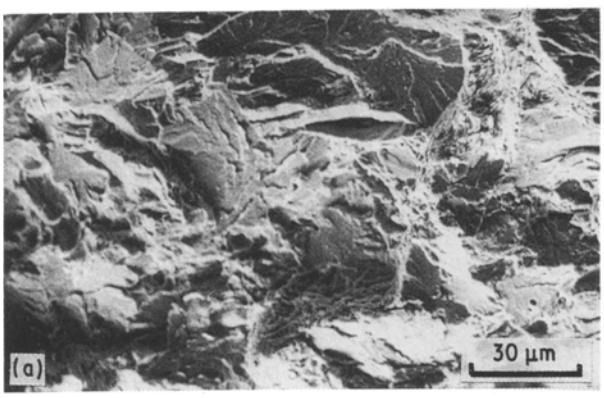

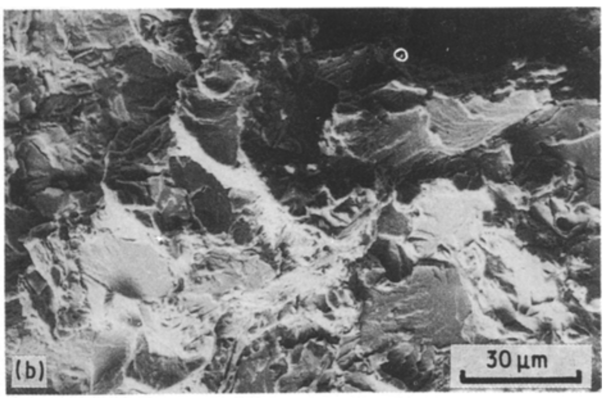

Figure 4 SEM fractographs of steel samples (a) 1B; (b) 2B; (c) 3B.

(Fig. 3a, b). Inclusion contents were however appreciably reduced after both NaCl and $CaCl_2$ treatments (Table II). Chemical analysis results (Table I) also indicate a positive reduction in aluminium and silicon contents after salt treatment.

Mechanical properties are reported in Tables III to V. SEM fractographs in Fig. 4 compare the tensile fracture characteristics of the three steels in the as-forged condition.

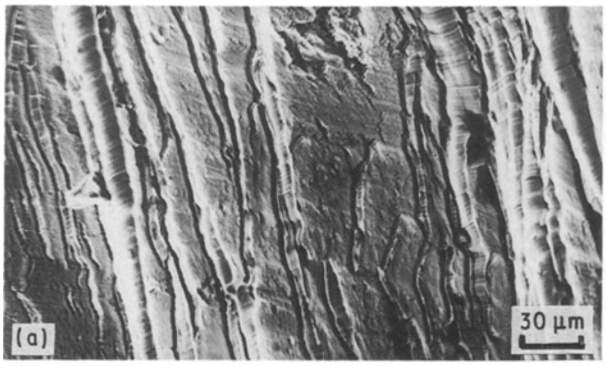

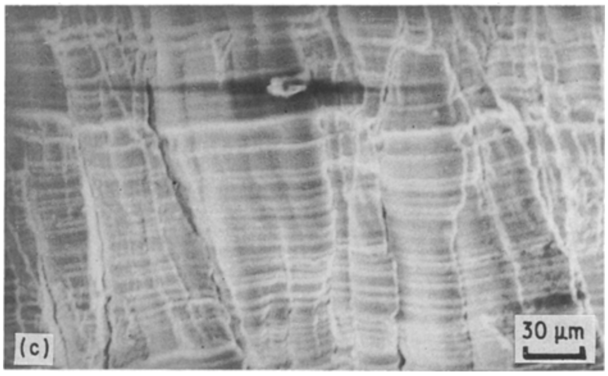

Figure 5 SEM micrographs of the undersides of chips (a) steel 1A; (b) 2A; (c) 3A.

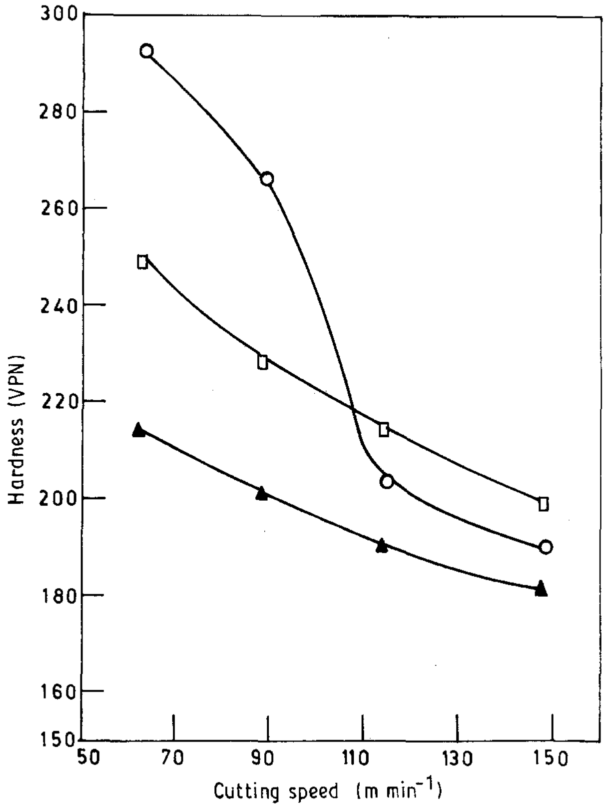

Figure 6 Microhardness (VPN) of chips as a function of cutting speed ○, 1A; □, 2A; ▲, 3A.

SEM photographs (Fig. 5a–c) of the undersized of the chips reveal the extent of cracking, folding and side flow in the chips of the three steels. Chips of steels 1A and 2A had undergone considerable folding. On the contrary, chips of steel 3A contained profuse microcracks and showed relatively less folding. The microhardness of the chips is plotted as a function of machining speed in Fig. 6. Chips of steel 3B had the lowest hardness.

4. Discussion

Examination of as-cast microstructures revealed graphite precipitation in steel 3B. The graphite was retained after water quenching from 900 °C. The presence of graphite particles was confirmed by electron microprobe analysis (Fig. 1a, b). Although the quantity of NaCl added to the melt in the present experiment was much greater than the dose added in an earlier experiment [3], the extent of graphitization was not large. Inclusion content was however appreciably reduced by treatment with chloride salts. The following mechanisms of inclusion removal are likely:

1. Chloride salts wet the inclusion particles, and as a result the particles can cluster together and float up.
2. Thermodynamic calculations suggest that the following reactions are possible at 1600 °C:

$$(Al_2O_3) + 2\{NaCl\} + 3\underline{C} = 2(AlCl) + 3\{CO\} + 2\,\underline{Na} \qquad (g)$$
$$\Delta G = -\text{ve}$$

$$(SiO_2) + 4\{NaCl\} + 2\underline{C} = (SiCl_4) + 2\{CO\} + 4\,\underline{Na} \qquad (s)$$
$$\Delta G = -\text{ve}$$

According to the above reactions, alumina and silica particles are converted to volatile AlCl and $SiCl_4$ phases and are removed from the melt. The actual reduction in residual silicon and aluminium contents in the melts following NaCl treatment (Table I) indicates that this may be the case. Further, it is likely that elemental Na released through such reactions is responsible for causing mild graphitization. The presence of such tiny graphite particles may account for the multiple cracks in the chips of steel 3B (Fig. 5c). Cracks are initiated at the graphite/matrix interface and propagate through the matrix, encouraging early chip break-up.

An evaluation of the mechanical properties of all three steels was carried out to assess the effect of chloride-salt treatment, if any. The slight reduction in the tensile and yield strength in the wrought samples after chloride-salt treatment may be attributed to the graphitization phenomenon. The $CaCl_2$-treated sample (2B) was distinctly inferior to the other two steels in terms of ductility. The tensile fracture in each sample was of the transgranular brittle type. The fractographs showed well-marked river patterns. However, the extent of brittleness of steel 2B was greater than that of either 1B or 3B. This is also clearly revealed by tensile fractographs in Fig. 4a–c. In steels 1B and 3B, crack initiation occurred at the grain boundary. In steel 2B, in addition to grain-boundary regions, crack initiation had occurred at numerous other points. The reasons for this difference are, however, not clear. The impact strength in steel 3B did not decrease at subzero temperatures (− 20 °C). Subzero treatment reduced impact strength appreciably in both steels 1B and 2B. It is probable that the impact transition temperature dropped quite appreciably following NaCl treatment due to removal of inclusions. This also improved transverse properties in steel 3B.

After 775 °C annealing, the ductility of the tensile test pieces of steel 3B was higher than that of 1A. The ductility was minimal in steel 2B in both hot-forged conditions and after 775 °C annealing. Partial spheroidization of pearlite in steel 3B after annealing at 775 °C obviously contributed to the improved ductility. However, it is not clear why similar structural modifications and improvements in ductility were not achieved in steel 2B. No clue was obtained from the microstructure. The formation of calcium aluminate inclusions and their precipitation at the grain boundaries may be a possible cause for deterioration of low-temperature toughness. The deep secondary cracks at the grain boundaries (Fig. 4b) also hint at this possibility. However, further work is necessary for elucidation of the phenomenon.

SEM examination of the underside of the chips revealed differences in the flow characteristics of the three steels. Appreciable folding of the chips occurred in 1A and 2A (Fig. 5a, b). The extent of chip folding was much less in 3A: the chips had cracked profusely (Fig. 5c). Although the trend of variation of microhardness of the chips with cutting force (Fig. 6) follows an identical pattern, it is noteworthy that the chips of 3A had the lowest hardness. The microstructure of a chip of 3A reveals a completely spheroidized structure (Fig. 2c) which is the cause of its relative softness. The multiple cracks in the chips of steel 3A (Fig. 5c) appear to be a result of partial graphitization of the steel. Cracks probably initiated from the graphite/matrix interface and then propagated through the matrix, causing fracture.

5. Conclusions

The inclusion content is hypereutectoid (1.0 % C) steel can be reduced considerably by treatment of the liquid steel with $CaCl_2$/NaCl in the transfer ladle. Considerable grain refinement occurs in hypereutectoid steels after treatment with $CaCl_2$/NaCl. The effect of NaCl is more conspicuous in this respect.

NaCl treatment of liquid steel also produces the following effects.

1. A small quantity of graphite is precipitated in the as-cast ingots. The graphite particles do not redissolve at 900 °C.
2. In hot-forged and air-cooled samples, as well as in samples normalized from 775 °C, pearlite is completely spheroidized without any special treatment.
3. Impact strength does not deteriorate even at − 20 °C, probably due to lowering of the impact transition temperature.

Acknowledgements

The authors would like to thank the director, RDCIS, SAIL, Ranchi for the provision of laboratory facilities. Thanks are also due to Dr S. Majumdar of RDCIS, SAIL, Ranchi, Professor A. B. Chattopadhyay of the Mechanical Engineering Department, IIT Kharagpur, and Mr S. Singh and Mr R. Ramakrishnan, former undergraduate students of IIT Kharagpur, for their assistance in the experimental work.

References

1. L. M. NIKETIN and N. S. KRESHCHANOVSKII, *Russian Casting Production* **6** (1967) 254.
2. A. S. KHARITONOV, I. I. Z. GUR'EV, N. I. SHANIN and L. T. IL'INKOVA, *Stal in English*, July (1970) 522.
3. D. MUKHERJEE, S. R. MEDIRATA, A. K. CHAKRABARTI and P. BANERJEE, *J. Mater. Sci. Lett.* **7** (1988) 43.
4. A. K. CHAKRABARTI, S. GEORGE, B. SHARMA, D. MUKHERJEE and R. N. MUKHERJEE, *J. Mater. Sci. Lett.* **6** (1977) 1145.

Received 2 January
and accepted 29 October 1990